

EUROPEAN ORGANIZATION FOR NUCLEAR RESEARCH

Addendum to the IS451 proposal

Shape coexistence in neutron-rich Sr isotopes: Coulomb excitation of ^{98}Sr

E. Clément^{1*}, A. Gørgen^{2*}, W. Korten², A. Obertelli², Ch. Theisen²,
P. Delahaye¹, G. de France¹, A. Dijon¹, B. Bastin¹, J. Cederkäll³, J. Pakarinen³,
F. Wenander³, D. Voulot³, T. Stora³, J. Ljungvall⁷, M. Zielińska⁴,
P. Napiorkowski⁴, K. Wrzosek⁴, P. Van Duppen⁵, M. Huyse⁵, S. Franchoo⁶,
F. Dayras⁷, G. Georgiev⁷, A. Ekström⁸, M. Guttormsen⁹, A.C. Larsen⁹, S. Siem⁹,
N.U.H. Syed⁹, P.A. Butler¹⁰, A. Petts¹⁰, D.G. Jenkins¹¹, V. Bildstein¹²,
R. Gernhäuser¹², T. Kröll¹², R. Krücken¹², J. Van de Walle¹³,
D. Mücher¹⁴, A. Blazhev¹⁴, N. Warr¹⁴, P. Reiter¹⁴

¹GANIL, Caen, France²Irfu/SPhN, CEA Saclay, France³Phy. Department PH-SME-IS, CERN, Geneva, Switzerland⁴Heavy Ion Laboratory, Warsaw, Poland⁵IKS Leuven, Belgium⁶IPN Orsay, France⁷CSNSM Orsay, France⁸Department of Physics, Lund University, Sweden⁹Department of Physics, University of Oslo, Norway¹⁰Oliver Lodge Laboratory, University of Liverpool, UK,¹¹Department of Physics, University of York, UK,¹²TU München, München, Germany¹³KVI, University of Groningen, Groningen, Netherlands¹⁴Institut für Kernphysik, Universität zu Köln, Köln, Germany

Spokespersons: E. Clément and A. Gørgen

Contactperson: J. Pakarinen

January 8, 2010

Abstract

In this addendum we ask for beam time to perform Coulomb excitation of ^{98}Sr in order to complete our program on the study of shape coexistence and evolution of collectivity in neutron rich strontium isotopes at $N=60$. In July 2007, we have performed the Coulomb excitation of ^{96}Sr at the Miniball beam line. At the time of the experiment the failure of the REX-Trap lowered the beam intensity compare to the proposal. In spite of a lower counting rate, we have significantly improved the measurement of the $B(E2,0_1^+ \rightarrow 2_1^+)$ and extracted for the first time the spectroscopic quadrupole moment of the first 2^+ state. Due to the

*co-spokesperson



low efficiency of the low energy part of REX in beginning of 2007, 10 over 24 shifts were deduced from the allocated beam time. We require **10 additional shifts** to fulfill the physics objective described in the original proposal and performed the Coulomb excitation of the highly collective ^{98}Sr .

Motivation

The evolution of the deformation in the Zr, Sr and Kr n-rich isotopes around $N=60$ has attracted many theoretical and experimental works since several decades. It has been established since many years that the neutron rich Sr and Zr isotopes are characterized by a sudden onset of quadrupole deformation at neutron number $N = 60$. This becomes evident already from the excitation energies of the first 2^+ states. Fig. 1 shows the dramatic drop in the excitation energy of the 2^+ states around $N = 60$ for both the Sr and Zr isotopes. Recently the systematic of the first 2^+ state was extended in the Kr chain up to $N=60$ [1]. At $N=60$, the energy of the first excited state drops down by almost 700 keV in the Sr and Zr isotopes and by 400 keV in the Kr isotopes. The so-called shape transition seems to be rather abrupt in the Kr case but this figure is in contradiction with a more gradual change of deformation deduced from laser spectroscopy and presented in figure 2. The study of the onset of deformation in the Kr chain is the purpose of the IS485 experiment defended by D. Müncher and collaborators. From the different works using laser spectroscopy technique, measurement of the energy of the first 2^+ state and $B(E2)$, one can extract in a model dependent way a deformation parameter β_2 . Disappearances on β_2 usually arise between the different extracted values as illustrated in [1] and [2] for the Kr, Sr and Zr chains and lead to confusing interpretation on the deformation. The differences are coming from the procedure used to estimate the deformation. As mentioned in [1], others effects as octupole correlation or skin thickness could explain the differences. An independent way to determine the algebraic deformation (prolate or oblate) is to measure the spectroscopic quadrupole moment of the 2_1^+ state by safe coulomb excitation as we are proposing.

The strong dependence of observed spectroscopic properties on the number of protons and/or neutrons makes of the $A \approx 100$ region a very challenging case for various theoretical models. From the microscopically point of view, the sudden shape change is associated to a sharp modification of the shell structure at $N=60$. Looking at the 2 neutrons separation energies compiled by AME2003 and the JYFLATRAP mass data base, one can notice at $N=58-60$ in Rb, Sr, Y and Zr isotopes a staggering of the value which is not observed in the other elements (see Fig. 2). This is an established indication of a profound shell modification associated to shell gap, intruder or extruder orbitals. In the deformed shell model approach, the onset of collectivity can be understood through a competition between the spherical gaps at $Z=38, 40$ and $N=56$, and the deformed subshell closures at $Z=38, 40$ and $N=60, 62$ and 64 . In the Sr and Zr isotopic chains, a spherical-to deformed transition takes place when going from 58 to 60 neutrons, thus when the $\nu g_{7/2}$ orbital is being filled.

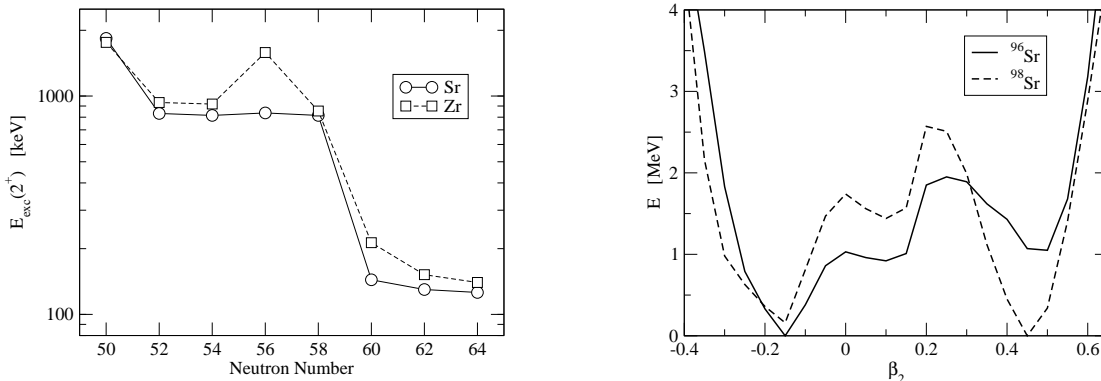


Figure 1: *Left*: Excitation energies of the 2_1^+ states for the chains of Sr and Zr isotopes. *Right*: Potential energy as a function of quadrupole deformation for ^{96}Sr and ^{98}Sr [12].

P. Federman and S. Pittel [9] proposed first to explain the shape transition through a strong $\pi - \nu$ interaction between the spin-orbit partner $1\pi g_{9/2}$ and $1\nu g_{7/2}$ but later experimental data refuted this hypothesis [3]. Then it was suggested that a significant correlation between $\pi 1g_{9/2}$ and $\nu 1h_{11/2}$ orbitals as the number of neutrons increases might have a role [4]. Finally it is often argued that this onset can be interpreted as a sudden decrease at $N=60$ of the occupancy of the proton orbital $1f_{5/2}$ and of the neutron $2d_{5/2}$

and $1g_{9/2}$ orbitals, accompanied by an increase of the occupancy of the $\pi 1g_{9/2}$ and $\nu 1h_{11/2}$ orbitals driving the deformation [5]. However looking at the values in the publication (Table II and III in [5]), significant modifications in the occupancy of other orbitals are also listed. In this last calculations, one can remark that both proton and neutron deformations increase at $N=60$. Recent experimental work on isomer spectroscopy in odd neutron Sr and Zr isotopes point the role of $\nu 9/2[404]$ extruder orbital as driver of the deformation at $N=60$ [6]. This is supported by the observation of $9/2^+$ isomeric state in ^{97}Sr , ^{99}Zr and ^{101}Zr interpreted as one-neutron hole excitation [6]. In this reference the authors describe the competition of spherical and deformed shell gaps generated by the $3/2[422]$, $3/2[411]$, the intruder $1/2[550]$, $3/2[541]$ ($h_{11/2}$ parentage) and extruder $9/2[404]$ neutron orbitals. Recently Shell Model calculations were performed in the Zr isotopic chain in an extended model space [7]. In this last work the interaction $\pi - \nu$ between the spin-orbit partner $1\pi g_{9/2}$ and $1\nu g_{7/2}$ was pointed back as the main mechanism for the shape modification: as the $\nu g_{7/2}$ orbital is being filled, the $Z=40$ subshell closure between the $1\pi f_{5/2}$ and $1\pi g_{9/2}$ effective single-particle energies (ESPE) is reduced. The $1\pi g_{9/2}$ ESPE has an increasing slope as the $1\pi f_{5/2}$ ESPE decreases more slowly when neutrons are added (see figure 1 in [7]). It is now established that this mechanism is responsible for the rapid onset of deformation in n-rich isotopes at $N=20$ and $N=28$ with different spin-orbit partners [8]. All these possible interpretations on the microscopic origin of the shape change clearly support the need for more spectroscopic informations like the spectroscopic quadrupole moment which is a very sensitive probe for calculations.

While theoretical calculations, for example using the Nilsson-Strutinsky method with Woods-Saxon potential [10], the relativistic mean field theory [11], or the Hartree-Fock-Bogoliubov approach with Gogny interaction [12] reproduce this onset of deformation qualitatively, they differ in the details of the deformation parameters and excitation energies. Most calculations predict slightly oblate ground-state deformations for the lighter isotopes and strongly deformed prolate shapes for the heavier ones. In the transitional region around $N = 60$ the different shapes are expected to coexist in a narrow energy range. Potential energy curves for ^{96}Sr and ^{98}Sr are presented in Fig. 1. The absolute minimum in ^{96}Sr is found to be oblate, while the strongly deformed prolate minimum is found about 1 MeV above. Oblate and prolate minima are almost degenerate in ^{98}Sr . This scenario is supported by the observation of excited 0^+ states at 1229 and 1465 keV in ^{96}Sr and at only 215 keV in ^{98}Sr . However, oblate shapes are difficult to prove experimentally, and so far there is no clear experimental evidence for oblate shapes in the neutron-rich Sr or Zr isotopes. Finally by comparing the different mean field approaches one can notice that calculations carried with axial symmetry predicted coexisting prolate and oblate minima with almost the same deformation. Calculations using more degree of freedom predict slightly oblate configuration coexisting with a large deformed prolate minimum [11] [10] [12]. Up to now there is no experimental proof for a large prolate or oblate deformation beyond $N=60$.

The nuclear structure of neutron rich Sr and Zr isotopes has been experimentally studied extensively in the past [3, 14–16]. Level schemes of ^{96}Sr and ^{98}Sr are shown in Fig. 3. In ^{96}Sr , the ground-state band has a vibrational-like character and previous $B(E2; 2_1^+ \rightarrow 0_1^+)$ value extracted from lifetime (7(4) ps [14]) was reported. Two low-lying 0^+ states were established by Jung *et al.* [17] at 1229 and 1465 keV and were interpreted as candidates for a deformed band head. An extremely strong electric monopole transition of $\rho^2(E0) = 0.18$ was observed between the 0_3^+ and 0_2^+ states [15, 18], indicating the presence of a sizeable deformation and strong mixing of the configurations. The sequence of the 0_3^+ (1465 keV), 2_3^+ (1629 keV), and 4_2^+ (1975 keV) states was interpreted as the well-deformed rotational band equivalent to the ground-state band in ^{98}Sr , even though the $2_3^+ \rightarrow 0_3^+$ transition remained unobserved. Lifetimes could be established for the 10^+ and 12^+ states in this band [3], from which a relatively small deformation of only $\beta_2 = 0.25$ was derived. It was argued that the 0_2^+ (1229 keV) and 2_2^+ (1506 keV) states form the low-spin members of this moderately deformed band, and it was concluded that the onset of deformation around $N = 58$ is not as abrupt as previously thought, but rather gradual [3]. The 0_3^+ and 2_3^+ states could still be interpreted as being based on a very deformed configuration, especially in the light of the strong $E0$ transition. However, the higher-spin members of such a structure, which are not observed, should then rapidly become yrast. The extremely strong $E0$ transition can only occur if the 0_2^+ and 0_3^+ states are strongly mixed, and the branching ratio of the transitions from the 4_2^+ state indicates also a strong mixing of the 2_2^+ and 2_3^+ states [16], so that the low-spin levels are displaced in energy and cannot easily be grouped into rotational bands. In odd neutron neighboring nuclei, many isomers based on single particle excitation were identified and quadrupole moment or deformation β_2 were extracted [3] [6] [19]. Mis-interpretations on the deformation of the ground

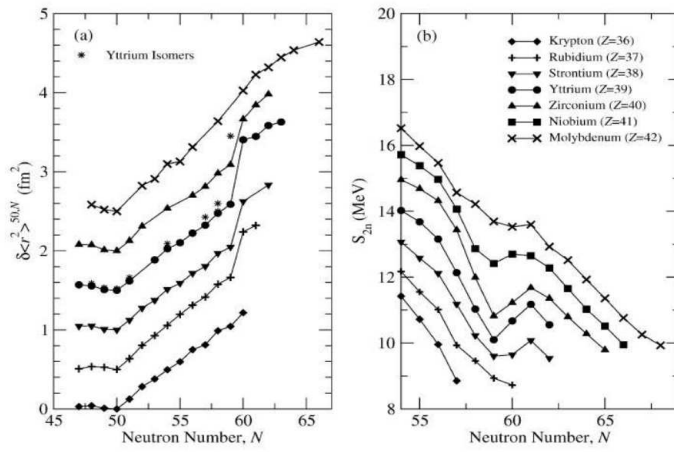


Figure 2: *left*: Measured mean-square charge radii as a function of the neutron number for $Z=36$ to 42. The sharp variation at $N=60$ is visible except for the Kr and Mo isotopes. *right* : 2 neutrons separation energy in the same nuclei as a function of the neutron number. The staggering of the value for Zr and Sr is visible at $N=58$. Picture taken from [13].

state arise due to the extrapolation of these higher lying states to the ground state structure. However it demonstrates that different deformations coexist at low energy in these nuclei around $N=60$ and meet the mean-field interpretation where different minima in the potential energy coexist.

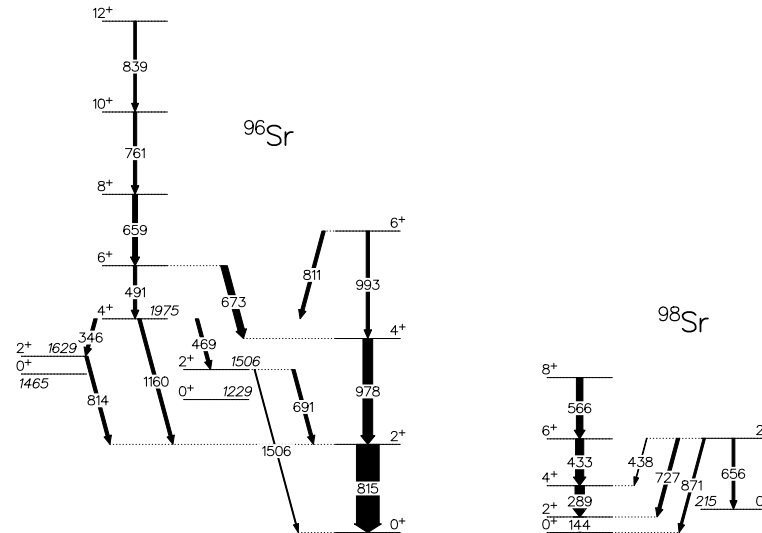


Figure 3: Partial level schemes of ^{96}Sr [3, 16] and ^{98}Sr [20].

Coulomb excitation of ^{96}Sr from July 2007 run

The aim of the 2007 run was to extract the electromagnetic properties of ^{96}Sr . A high quality beam, free from any contaminant, was delivered by the REX-ISOLDE accelerator at 2.87 MeV/A. The use of the SrF^+ molecule at the UC_x primary target and then broken in the EBIS charge breeder allow us to suppress the Rb contaminant (see Fig. 4). Yield measurements were performed on-line: $3.7 \cdot 10^5 \text{ } ^{96}\text{Sr}^{19}\text{F}^+/\mu\text{C}$ and $1.3 \cdot 10^5 \text{ } ^{98}\text{Sr}^{19}\text{F}^+/\mu\text{C}$ were obtained respectively.

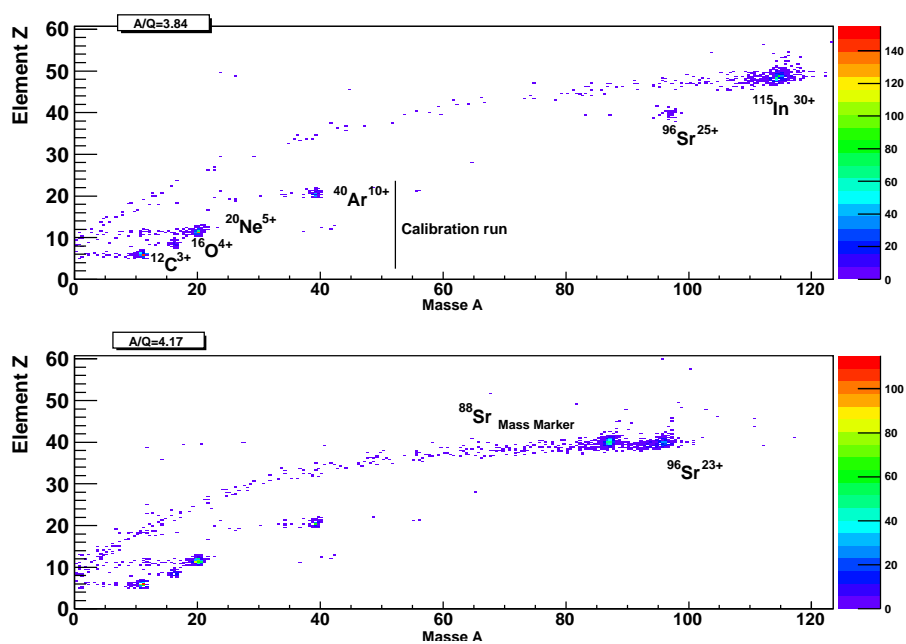


Figure 4: *Top* : Calibrated Bragg chamber 2D matrix for a REX setting at $A/Q = 3.84$ at the Miniball secondary target. The x-axis represents the mass A based on the total energy measurement. The y-axis represents the Z protons measurement based on the Bragg peak slope. An unique contaminant of ^{115}In is present and correspond to the total mass of the $^{96}\text{Sr}^{19}\text{F}$ molecule. *Bottom* : Calibrated Bragg chamber 2D matrix for a REX setting at $A/Q = 4.17$. The In contaminant is suppressed. The mass marker ^{88}Sr and stable $A/Q = 4$ ions from the EBIS were added to the matrix for calibration and self consistent checking. The last setting, free from any contaminant, was used in the present experiment.

However, due to a general failure of the REX-TRAP, radioactive beam was continuously injected in the EBIS charge breeder and lead to a low efficiency of about 1.9% of the low energy part of REX-ISOLDE. Moreover, 83% of the MINIBALL array was operational at the time of the experiment. Consistent measurements based on the global efficiency of the accelerator measured with stable marker and the excitation of the target at MINIBALL lead to an intensity of 0.5 to 1.0 10^4 pps for ^{96}Sr . In spite of the relative low beam intensity, Coulomb excitation on 2 different targets was successfully achieved. The corresponding spectra are presented in figure 5.

In both spectra, the $2_1^+ \rightarrow 0_1^+$ transition in ^{96}Sr is observed as well as the deexcitation of the target. In the case of the heavier target a weak transition corresponding to the 0_2^+ decay is visible in the insert. Combining the 2 different targets data set and the differential coulomb cross section as global input of the GOSIA code, we have significantly improved the measurement of the $B(E2, 0_1^+ \rightarrow 2_1^+)$ and extracted for the first time the spectroscopic quadrupole moment of the first 2^+ state. The experimental sensitivity of our measurement on the diagonal matrix element is illustrated in the figure 6. As a result, the matrix elements presented in table 1 were extracted from observed and unobserved transitions.

Table 1: Preliminary matrix elements obtained from the Coulomb excitation of ^{96}Sr .

Matrix element	measured value [eb]
$2_1^+ \rightarrow 0_1^+$	$-0.52 \begin{smallmatrix} (+0.09) \\ (-0.13) \end{smallmatrix}$
$4_1^+ \rightarrow 2_1^+$	≤ -0.75
$0_2^+ \rightarrow 2_1^+$	$0.19 \begin{smallmatrix} (+0.01) \\ (-0.01) \end{smallmatrix}$ [14]
$2_2^+ \rightarrow 0_1^+$	≤ 0.12
$2_1^+ \rightarrow 2_1^+$	$0.07 \begin{smallmatrix} (+0.39) \\ (-0.34) \end{smallmatrix}$

From the measurement of the spectroscopic quadrupole moment a weak static deformation can be assigned to the first excited state. For indication, using the deformed liquid drop model, one can extract $\beta \leq 0.14$. The mean deformation of the first 2^+ state is null as its $B(E2)$ is rather large (20 W.u) supporting a quasi-vibrator character for the ^{96}Sr in its ground state band structure. This deformation is also compatible

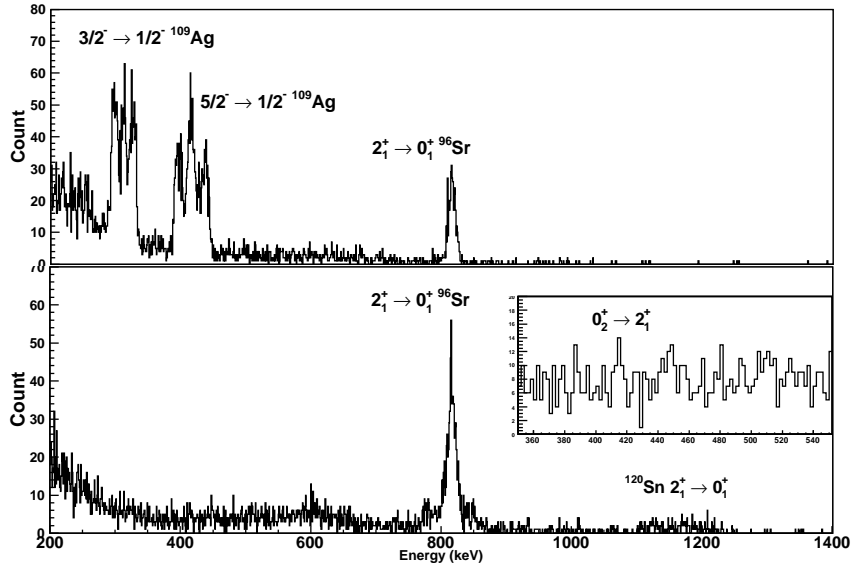


Figure 5: *Top* : Part of the gamma-ray spectrum detected in MINIBALL, Doppler corrected for the projectile, following the deexcitation of a ^{96}Sr beam impinging on a ^{109}Ag target. *Bottom* : Part of the gamma-ray spectrum detected in MINIBALL following the deexcitation of a ^{96}Sr beam impinging on a ^{120}Sn target. The insert shows a zoom on the weak $0_2^+ \rightarrow 2_1^+$ gamma decay.

with the moderate oblate deformation in the ground state calculated in the triaxial mean-field approach. At low excitation energy and low spins one expects the $(\nu d_{5/2})^2$ and/or $(\pi f_{5/2})^2$ multiplet, with $j=0,2,4$ configuration. The relatively high $B(E2)$ support a major protons contribution in the first 2^+ state. By opposition to the spherical Zr and Mo isotopes in which $(\pi g_{9/2})^2$ yrast multiplet are observed up to spin $I=8$, in ^{96}Sr the yrast 6^+ state built on top of the ground state is not fairly assigned and support the interpretation of a $(\pi f_{5/2})^2$ multiplet. Large scale Shell Model calculations are currently performed with the same configuration as the Zr study [7].

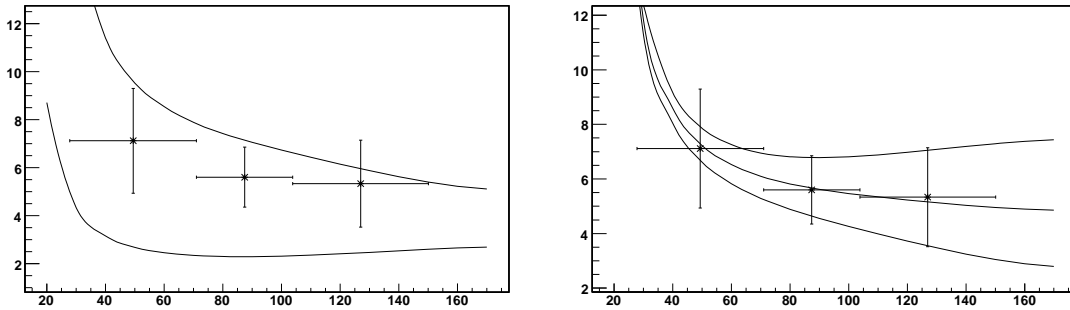


Figure 6: The x-axis represents the scattering angle in the center of mass. The y-axis represents the $2_1^+ \rightarrow 0_1^+$ intensity in ^{96}Sr normalized to the $2_1^+ \rightarrow 0_1^+$ intensity in the ^{120}Sn target. The experimental points are extracted from the present work. *Left*: The continuous lines delimit the surface corresponding to the previous lifetime measurement : 7(4) ps [14]. *Right*: The continuous lines are extracted from the present work : the center line corresponds to a lifetime of 4.1 ps and a spectroscopic quadrupole moment equal 0. The two extreme lines correspond to the same lifetime ($B(E2)$) and the spectroscopic quadrupole moment compatible with a diagonal matrix element equal to -0.5 and 0.5 eb respectively. Adding the data from the Coulomb excitation on the Ag target in a global GOSIA minimization lead to the results describe in table 1.

In ^{98}Sr , one can expect a different scenario. Beyond $N=60$, the highly collective rotational ground-state band of ^{98}Sr points to a large ground-state deformation and the 0_2^+ state at 215 keV, which decays to the ground state via an enhanced $E0$ transition of $\rho^2(E0) = 0.053$ [20], supports the scenario of shape coexistence with a high mixing. However, the rotational ground-state band follow almost a perfect rigid rotor in opposition with a large mixing of the wave function which should disturb the sequence. The measurement of the spectroscopic quadrupole moment in the ground state band will allow to *i*) extract the deformation and its sign (prolate or oblate), *ii*) check the validity of the perfect rigid rotor by comparing the spectroscopic quadrupole and its equivalent extracted from the $B(E2)$. Finally the measurement of the matrix elements related to the 2_2^+ state will infirm or not the interpretation of a configuration inversion between ^{96}Sr and ^{98}Sr by comparison. Moreover, direct extraction of the mixing angle between 0^+ and 2^+ states will be performed if enough statistics.

Experimental details

From the 2007 run, we have extracted the production yield mentioned in the previous section for both ^{96}Sr and ^{98}Sr . We would like to run with the same production scheme for ^{98}Sr and post-accelerate the radioactive ions at 2.9 MeV/A using the REX Linac. Assuming the REX-TRAP at its nominal value, we might expect a transmission higher by a factor 3 compare to the previous run. We believe that the improvement in statistical error for ^{96}Sr will not lead to an improvement in the physics conclusion. For the $2_1^+ \rightarrow 0_1^+$ matrix element, the relative error will change from 20% to 14% as the upper limit for the $2_1^+ \rightarrow 2_1^+$ matrix element will not be significantly changed. Assuming the Coulomb excitation cross section extracted from the matrix elements presented in table 1 and normalized to the $2_1^+ \rightarrow 0_1^+$, less than 10 counts can be expected for the 2_2^+ decay. On the other hand, a factor 3 more transmission in REX-ISOLDE lead to a equivalent post-accelerated intensity for ^{98}Sr compare to ^{96}Sr in 2007. We propose to focus our experiment on the measurement of the spectroscopic quadrupole moment in the ground state band of ^{98}Sr and try to populate the second 2^+ state.

We propose to use a secondary ^{208}Pb target for the Coulomb excitation of the projectiles. This choice is a compromise between the Coulomb excitation cross section for the second 2^+ state, the sensitivity to the sign of the deformation in the ground state band and the mass asymmetry for a better distinction in energy between scattered projectiles and target recoils in the charged particle detector. The prompt γ rays emitted after Coulomb excitation will be detected in the MINIBALL spectrometer of germanium detectors in coincidence with the scattered particles detected in an annular segmented silicon-strip detector. The silicon detector (CD) covers scattering angles between 16.3° and 53.3° in the laboratory frame. The detection of scattered projectiles corresponds to a range of scattering angles between 24° and 75° in the center-of-mass frame, whereas the detection of the recoiling target covers the range $73^\circ \leq \theta_{cm} \leq 148^\circ$. Both projectile and target will be detected in the overlapping range. The excitation probabilities will be normalized to the $2_1^+ \rightarrow 0_1^+$ transition since the value is precisely known [21]. The analysis will be performed using the code GOSIA [22, 23] to determine the set of transitional and diagonal matrix elements that best describes the observed γ -ray yields in a χ^2 minimization.

Coulomb excitation calculations and rate estimates

In order to evaluate the feasibility of the experiment we have performed Coulomb excitation calculations based on the known spectroscopic informations and different hypotheses for the collectivity of the states. The known spectroscopic parameters for the low-lying states in ^{98}Sr are listed in table 2. For estimation the lifetime of the 6_1^+ was extracted from the systematic of the ground state band. One can notice that the second 2^+ state is not yet firmly established. We have used the $B(E2)$ extracted from ^{96}Sr as assumption of its collectivity.

This can be translated in cross section as presented in table 3. Assuming 10^4 ^{98}Sr per second and a $1\text{mg}/\text{cm}^2$ ^{208}Pb target, we might expect the following yields for the different transitions presented in table 4. Cross sections are rather large as expected for a highly deformed nuclei. Consequently the excitation of the ground state band should be easily observed. The observation of the decay of the 2_2^+ state requires a full week of irradiation. As underlined in the table, we reach almost the same cross section between the 2_1^+ in ^{96}Sr and the 6_1^+ in ^{98}Sr . The sensitivity to the diagonal matrix element, assuming an equality between the diagonal and transitional matrix element, is indicated in the third line for each state. We strongly believe that we can extract the spectroscopic quadrupole moment in the 4_1^+ and 6_1^+ states. The count rate estimate

Table 2: Experimentally known lifetimes [ENSDF]

I_i	τ	I_f	E_γ [keV]
2_1^+	2.78(8) ns	0_1^+	144
4_1^+	80(8) ps	2_1^+	289
8_1^+	3.0(5) ps	6_1^+	565
10_1^+	1.07(17) ps	8_1^+	689
0_2^+	22.8 (19) ns	2_1^+	71
2_2^+		0_1^+	(871)

Table 3: Estimate of the Coulomb excitation cross sections in **barn** assuming different combinations of signs for the quadrupole moments of the 2_1^+ , 4_1^+ , 6_1^+ and 8_1^+ states. A negative sign corresponds to an oblate shape and positive sign to a prolate shape. Coulex cross section for ^{96}Sr are also presented for comparison.

I^π	2_1^+	4_1^+	6_1^+	8_1^+	0_2^+	2_2^+
prolate GSB	15.2	2.6	0.53	0.109	1	0.058
oblate GSB	16.2	3.7	0.92	0.06		
sensitivity	6%	42%	75%	81%		
^{96}Sr	1.7	0.04			0.01	0.02

was carefully checked according to our previous measurement. Looking at the digital clock of the Miniball electronics, we have effectively acquired 109 hours irradiation time with the Sn target. Assuming the cross sections calculated in table 1 for the ^{96}Sr , 10^4 pps and the absolute efficiency of Miniball, we obtain exactly the experimental statistics for the $2_1^+ \rightarrow 0_1^+$ transition.

Table 4: Estimated γ intensities using the assumptions described in the text.

I_i	I_f	E_γ [keV]	counts/day
2_1^+	0_1^+	144	11000
4_1^+	2_1^+	289	800
6_1^+	4_1^+	433	160
8_1^+	6_1^+	565	140
2_2^+	2_1^+	(727)	6
2_2^+	0_1^+	(871)	4

In order to reach the physics objectives, we would like to run during 24 UT beam time as required in the original proposal for each nucleus. Therefore, we ask for 10 additional shifts for the present addendum. A couple of UT might be used by the ISODLE operators to optimize the production in order to reach a rather constant yield of 10^4 pps at Miniball. Optimization on the pressure of the buffer gas in the target might be investigated.

Summary

We propose to study the shape evolution and shape coexistence in the neutron-rich Sr isotopes through Coulomb excitation of ^{98}Sr . Both transitional and diagonal matrix elements will be determined in a differential Coulomb excitation measurement utilizing the reorientation effect. The static quadrupole moments of states in the rotational ground state band will shed light on shape coexistence and shape evolution in the mass region. Comparison with the data obtained in ^{96}Sr will give important constraints for modern nuclear structure theories describing such phenomena. **We ask for 10 additional shifts of ^{98}Sr beam to perform the proposed experiment in 24 shift units.**

Beam requirements						
Beam	Min. intensity (REX)	Target	Ion Source	Remaining shifts	Additional requested	Total
^{98}Sr	10^4 pps	$\text{UC}_x / \text{ThO}_2$	Positive surface	14	10	24

References

- [1] N. Marginean *et al.*, Phys. Rev. C 80, 021301(R) (2009)
- [2] M. Keim *et al.*, Nucl. Phys. A 586 (1995)
- [3] W. Urban *et al.*, Nucl. Phys. A 689 (2001)
- [4] P. Federman, S. Pittel, Phys. Lett. B 77, 29 (1978)
- [5] A. Kumar and M. R. Gunye Phys. Rev. C 32, 2116 (1985)
- [6] W. Urban *et al.*, Eur. Phys. J. A 22,241 (2004)
- [7] K. Sieja *et al.*, Phys. Rev. C 79, 064310 (2009)
- [8] O. Sorlin and M.-G. Porquet Prog.in Part. and Nucl. Phys. 61, 602 (2008)
- [9] P. Federman, S. Pittel, Phys. Lett. B 69, 385 (1977)
- [10] J. Skalski, S. Mizutori, W. Nazarewicz, Nucl. Phys. A 617, 282 (1997)
- [11] G.A. Lalazissis, M.M. Sharma; Nucl. Phys. A 586, 201 (1995)
- [12] S. Hilaire, M. Girod;
http://www-phynu.cea.fr/science-en-ligne/carte_potentiels_microscopiques/carte_potentiel_nucleaire.htm
- [13] F.C. Charlwood *et al.* Phys. Lett. B 674, 23 (2009)
- [14] H. Mach *et al.*, Nucl. Phys. A 523,197 (1991)
- [15] G. Lhersonneau *et al.*, Phys. Rev. C 49, 1379 (1994)
- [16] C.Y. Wu *et al.*, Phys. Rev. C 70, 064312 (2004)
- [17] G. Jung *et al.*, Phys. Rev. C 22, 252 (1980)
- [18] K. Kawade *et al.*, Z. Phys. A 304, 293 (1982)
- [19] T. Rzaca-Urban *et al.*, Phys. Rev. C 79, 024319 (2009)
- [20] Nucl. Data. Sheets 98, 335 (2003)
- [21] H. Mach *et al.*, Phys. Lett. B 230, 21 (1989)
- [22] D. Cline, Ann. Rev. Nucl. Part. Sci. 36, 683 (1986)
- [23] T. Czosnyka, GOSIA2, 2005, MINIBALL User's Workshop 2005